

Statistical properties of curved polymer

SURYA KANTA GHOSH* and ANIRBAN SAIN

Department of Physics, Indian Institute of Technology Bombay, Mumbai 400 076, India

*Corresponding author. E-mail: surya@phy.iitb.ac.in

Abstract. Intrinsic curvature of biopolymers is emerging as an essential feature in various biological phenomena. Examples of polymers with intrinsic curvature are microtubule in eukaryotic cells or FtsZ filaments in prokaryotic cells. We consider the general model for polymers with intrinsic curvature. We aim to study both equilibrium and dynamic properties of such polymers. Here we report preliminary results on the equilibrium distribution function $P(\mathbf{R})$ of the end-to-end distance \mathbf{R} . We employ transfer matrix method for this study.

Keywords. Intrinsically curved polymer; end-to-end distance vector.

PACS Nos 87.15.He; 87.16.Ka; 36.20.Ey; 82.35.Pq

1. Introduction

Naturally occurring semiflexible polymers are commonly found in various biological systems. Some examples are double stranded DNA (dsDNA), actin, microtubule in the increasing order of bending stiffness. Equilibrium and non-equilibrium statistical properties of such polymers have been an active area of research since last decade. Recently, it has been discovered that some of the semiflexible biopolymers have intrinsic curvatures. Examples are microtubules [1] in animal cells, FtsZ filaments in bacteria [2] and even dsDNA [3]. The difference is that unlike the common semiflexible polymers which have straight filament configurations in their ground states, a polymer with intrinsic curvature attains lowest energy when it has a specified radius of curvature R_0 . At finite temperature, thermal fluctuations around the respective ground states decide the conformational statistics of the polymer. For semiflexible polymers, the relevant non-dimensional quantity is l_p/L , where l_p is the persistence length (which is proportional to the bending modulus k) and L is the contour length of the polymer. In the limit, $l_p/L \ll 1$, the polymer behaves as a flexible polymer whereas in the limit $l_p/L \geq 1$ it behaves like a straight rod. For polymers with intrinsic curvature there is an additional length scale R_0 . Interplay of this length scale with l_p and L will be interesting to study. For example, when bending rigidity is very high and R_0 is small then the polymer will circle around itself and the end-to-end distance of the polymer will vary between zero and the diameter πR as L increases. The effect of thermal fluctuation adds further richness

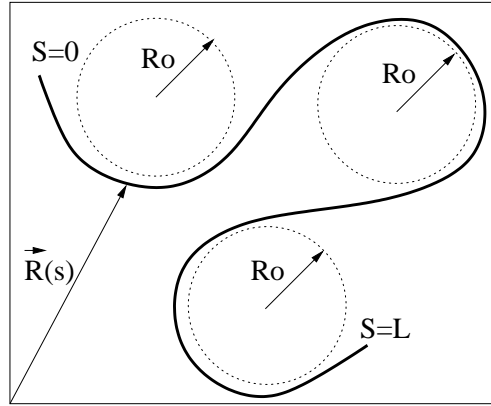


Figure 1. Intrinsically curved polymer with radius of curvature R_0 .

to this structure. In this brief report we describe our method of computing the distribution function of the end-to-end distance $P(R)$ and present some preliminary results.

2. The model

The polymer of length L is represented by a space curve $\mathbf{R}(s)$ (figure 1), where parameter $s \in [0, L]$. If the local radius of curvature is $r(s)$ then the curvature is defined as $C(s) = (1/r(s)) = |d^2\mathbf{R}(s)/ds^2|$.

Here $|d^2\mathbf{R}(s)/ds^2|$ is the derivative of the tangent vector at the point $\mathbf{R}(s)$. If the system has an intrinsic radius of curvature R_0 then the Hamiltonian H [4] is given by

$$H = k \int_{s=0}^L \left(\left| \frac{d^2\mathbf{R}(s)}{ds^2} \right| - \frac{1}{R_0} \right)^2 ds, \quad (1)$$

where k is the bending modulus.

In the discrete limit the monomers are given by the position vector \mathbf{R}_i and in units of bond length, the bond vectors are $\hat{t}_i = \mathbf{R}_{i+1} - \mathbf{R}_i$. Then the Hamiltonian in the discretized form can be written as

$$H = k \sum_{i=1}^{N-1} \left\{ \sqrt{2(1 - \hat{t}_i \cdot \hat{t}_{i+1})} - \frac{1}{R_0} \right\}^2. \quad (2)$$

The distribution function $P(\mathbf{R})$ of the end-to-end vector $\mathbf{R} = \sum_{i=1}^N \hat{t}_i$ is given by [5]

$$P(\mathbf{R}) = C \int d\hat{t}_1 \cdots \int d\hat{t}_N e^{-\beta H} \delta \left(\sum_{i=1}^N \hat{t}_i - \mathbf{R} \right), \quad (3)$$

where C fixes $\int d\mathbf{R}P(\mathbf{R}) = 1$. With one end of the polymer at $\mathbf{R} = 0$, the probability $p(z)$ for the other end to be in a given z plane is related to $P(\mathbf{R})$ through the expression $p(z) = \int d\mathbf{R}P(R)\delta(R_3 - z)$, where $\mathbf{R} = R_1\hat{x} + R_2\hat{y} + R_3\hat{z}$. Defining a generating function $\tilde{p}(f) = \int_{-L}^L dz \exp(fz/l_p)p(z) = Z(f)/Z(f=0)$, where $l_p = 2k/k_B T$ and $Z(f)$ is

$$Z(f) = \int dt_1 \cdots \int dt_N \exp \left[-\beta H + \frac{f}{l_p} \sum_{i=1}^N \hat{t}_i^z \right]. \quad (4)$$

Substituting the Hamiltonian in the above expression, the discretized form of $Z(f)$ is

$$\begin{aligned} Z(f) &= \sum_{\hat{t}_1} \cdots \sum_{\hat{t}_N} \exp \left\{ -\beta k \sum_{i=1}^{N-1} 2(1 - \hat{t}_i \cdot \hat{t}_{i+1}) \right\} \\ &\times \exp \left[-\beta k \left\{ -2\sqrt{2}\sqrt{(1 - \hat{t}_i \cdot \hat{t}_{i+1})} \left(\frac{1}{R_0} \right) + \left(\frac{1}{R_0} \right)^2 \right\} \right] \\ &\times \exp \left[\frac{f}{2l_p} \left\{ \sum_{i=1}^{N-1} (\hat{t}_i + \hat{t}_{i+1}) \cdot \hat{z} + (\hat{t}_1 + \hat{t}_N) \cdot \hat{z} \right\} \right]. \end{aligned} \quad (5)$$

$Z(f)$ can be computed using transfer matrices [5].

$$Z(f) = \sum_{\hat{t}_1} \sum_{\hat{t}_N} \langle \hat{t}_1 | V^{N-1} | \hat{t}_N \rangle \exp \left\{ \frac{f}{2l_p} (\hat{t}_1 + \hat{t}_N) \cdot \hat{z} \right\}, \quad (6)$$

where the matrix elements are

$$\begin{aligned} \langle \hat{t}_i | V | \hat{t}_{i+1} \rangle &= \exp \left[-\beta k \left\{ 2(1 - \hat{t}_i \cdot \hat{t}_{i+1}) - 2\sqrt{2}\sqrt{(1 - \hat{t}_i \cdot \hat{t}_{i+1})} \left(\frac{1}{R_0} \right) \right\} \right] \\ &\times \exp \left[-\beta k \left(\frac{1}{R_0} \right)^2 + \frac{f}{2l_p} (\hat{t}_i + \hat{t}_{i+1}) \cdot \hat{z} \right]. \end{aligned} \quad (7)$$

Once $Z(f)$ is known, $\tilde{P}(f)$ and $p(z)$ can be computed. Finally, using tomographic method [6] we obtained the expression for $P(\mathbf{R})$ as

$$P(\mathbf{R}) = -\frac{1}{2\pi z} \frac{dP(z)}{dz} \Big|_{z=R}. \quad (8)$$

We allow fluctuations of all the tangent vectors, including the two end vectors, i.e., free boundary conditions. In the high R_0 limit the main contribution to $Z(f)$ comes from configurations where the interbond angles are small. But the dimension of the transfer matrix V depends on the number of bins in which the angular space (θ_i, ϕ_j) is divided. This is numerically very expensive since the binning has to be dense enough to pick up the contribution from the small interbond angles. We therefore vary \hat{t}_i over the whole angular space but restrict \hat{t}_{i+1} to vary within a

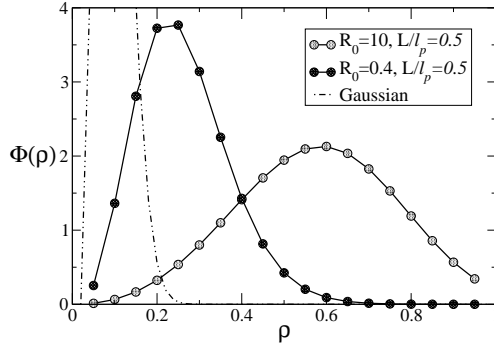


Figure 2. End-to-end distance of a polymer with large l_p .

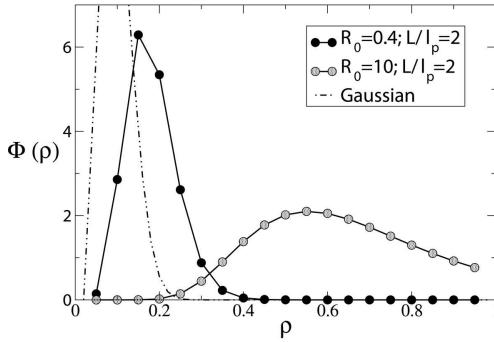


Figure 3. End-to-end distance of a polymer with small l_p .

narrow cone. This cone is densely binned whereas the angular binning for \hat{t}_i is not so dense. This truncated space for the relative angle between \hat{t}_i and \hat{t}_{i+1} picks up the major contribution. Using this scheme we have been able to verify the large l_p/L limit of the semiflexible chain. We now report our preliminary results for $P(R)$ for the chain with intrinsic curvature.

3. Results and discussions

We present results for $P(R) \equiv \phi(\rho)$ in terms of the scaled variable $\rho = R/L$. For an intrinsically curved polymer the energy per unit length in $k_B T$ units is given by

$$\frac{1}{L} \left(\frac{H}{k_B T} \right) = (l_p/L) \int_0^L \left(\frac{1}{R} - \frac{1}{R_0} \right)^2 ds, \quad (9)$$

i.e, the energy per unit length is proportional to l_p/L .

At large l_p/L , little deviation of R from R_0 makes the energy cost for such a configuration large. This will push the peak of $\phi(\rho)$ away from the Gaussian peak and force the polymer to make circular arcs of radius R_0 . Larger the value of R_0

larger will be the most probable value of R . This trend is visible in figure 2 where l_p is large. By the same argument, for small values of l_p/L the fluctuations of R around R_0 will be less costly and hence the behaviour will be dominated by the flexible limit and the peak of $\phi(\rho)$ moves towards the Gaussian peak. This trend is visible in figure 3.

Note that at large l_p/L the position of the peak of $\phi(\rho)$ also depends on L . We expect that for L equal to odd multiples of πR_0 the peak will be at $\pi R_0/L$ whereas for even multiples it will move towards zero. We are yet to verify these expectations.

Acknowledgments

We thank Dr D Das for discussions.

References

- [1] E Grishchuka, M Molodtsov, F Ataulakhanov and J McIntosh, *Nature (London)* **438**, 384 (2005)
- [2] J Mingorance *et al*, *J. Biol. Chem.* **280**, 20909 (2005)
- [3] J Moukhtar *et al*, *Phys. Rev. Lett.* **98**, 178101 (2007)
- [4] R Goldstein and S Langer, *Phys. Rev. Lett.* **75**, 1094 (1995)
- [5] P Ranjit, P Kumar and G I Menon, *Phys. Rev. Lett.* **94**, 138102 (2005)
- [6] J Samuel and S Sinha, *Phys. Rev.* **E66**, 050801(R) (2002)